Large Tunnel Magnetoresistance in Epitaxial Oxide Spin-Filter Tunnel Junctions

Takayuki Harada, Isao Ohkubo, Mikk Lippmaa, Yasuaki Sakurai, Yuji Matsumoto, Shunsuke Muto, Hideomi Koinuma, and Masaharu Oshima*

A high-performance spin filter tunnel junction composed of an epitaxial oxide heterostructure is reported. By independently controlling the magnetic orientations of ferromagnetic tunnel barrier and electrode layers, a tunnel magnetoresistance ratio exceeding 120% is obtained purely by the spin filtering effect. A newly introduced spin filter material, $Pr_{0.8}Ca_{0.2}Mn_{1-y}Co_yO_3$, is shown to be useful for building novel multibarrier spintronic tunnel devices due to its composition-controlled magnetic hardness.

1. Introduction

Developments in nanotechnology have made it possible to use quantum tunneling of electrons across a nanometer-thick insulator for device applications, e.g. magnetic random access memories, hard disk read-and-write head, magnetic field sensors, etc. In conventional tunnel junctions, a nonmagnetic insulator (NI) tunnel barrier acts as a passive separator between two electrodes. For example, in tunnel magnetoresistance (TMR) and Josephson junctions, the device functionalities are derived from the properties of the ferromagnetic or superconducting electrodes. If a functional material with nonlinear magnetic, dielectric or multiferroic properties[1–3] is employed as a tunnel barrier, the tunneling probability of electrons may be affected by the characteristics of the tunnel barrier material itself. A spin filter junction is a particularly good demonstration, where a ferromagnetic insulator (FI) tunnel barrier between non-ferromagnetic electrodes is responsible for producing a spin-polarized flow of tunneling electrons.[1,2,4–9] In spintronic applications, such junctions can be used to inject a spin-polarized current into a semiconductor device.[9,10] The operation of a spin-filter tunnel junction is based on spin-dependent tunneling through a thin FI layer. Due to an exchange splitting (Δ_{EX}) in the FI layer, the effective barrier height for tunneling electrons depends on the spin orientation, as shown in a simplified band diagram in **Figure 1**a, right. A spin-polarized current arises due to preferential tunneling of up-spin electrons through the junction. The operation of a spin filter can be verified by observing TMR in a normal metal (NM)/FI/ferromagnetic metal (FM) structure, i.e., combining a spin-filter tunnel junction (SFTJ) with a ferromagnetic spin detector in a single device. In this structure, the junction resistance is dependent on the parallel (P) or antiparallel (AP) magnetic configurations of the FI and FM layers. The effectiveness of the spin filter element can be determined by looking at the contrast between the P and AP-state currents, i.e., the TMR ratio, which we define as $TMR = (R_{AP} - R_P)/R_P$, where R_P and R_{AP} are the junction resistances in the parallel and antiparallel states, respectively. Although SFTJs have been actively studied,[2,5,7,9] achieving a large TMR response remains elusive, and spin filtering effects have been reported only in a limited number of materials, such as Eu calcogenides[1,4,11] and few oxides.[2,7,12] The main difficulty in obtaining high spin filtering efficiency appears to be due to the degradation of ferromagnetism in the FI layer that is only a few nanometers thick.[13] A major technical problem in a spin filter-detector junction is the magnetic coupling between the spin-filter tunnel barrier and a ferromagnetic spin detector electrode, which prevents independent control of the magnetic orientations of the two layers, leading to difficulties in measuring the true spin contrast of the spin-filtered tunneling electrons.

Dr. T. Harada,[+] Prof. I. Ohkubo,[++] Y. Sakurai, Prof. M. Oshima
Department of Applied Chemistry
The University of Tokyo
7-3-1, Hongo, Bunkyo-ku, Tokyo, 113-8656, Japan
E-mail: ohkubo@sr.t.u-tokyo.ac.jp
Prof. M. Lippmaa
Institute for Solid State Physics
The University of Tokyo
5-1-5, Kashiwanoha, Kashiwa, Chiba, 277-8581, Japan
Prof. Y. Matsumoto
Materials and Structures Laboratory
Tokyo Institute of Technology
4259, Midori-ku Nagatsuta, Yokohama, 226-8503, Japan
Prof. S. Muto
Department of Materials, Physics, and Energy Engineering
Graduate School of Engineering Nagoya University
Nagoya, 464-8603, Japan
Prof. H. Koinuma
Graduate School of Frontier Sciences
The University of Tokyo
5-1-5, Kashiwanoha, Kashiwa, Chiba, 277-8568, Japan
[+] Present address: Institute for Solid State Physics, The University of Tokyo, 5-1-5, Kashiwanoha, Kashiwa, Chiba, 277-8581, Japan
[++] Present address: National Institute for Materials Science, 1-1 Namiki Tsukuba-shi, Ibaraki 305-0044, Japan; OHKUBO.Isao@nims.go.jp

DOI: 10.1002/adfm.201200985

ADVANCED FUNCTIONAL MATERIALS
www.afm-journal.de

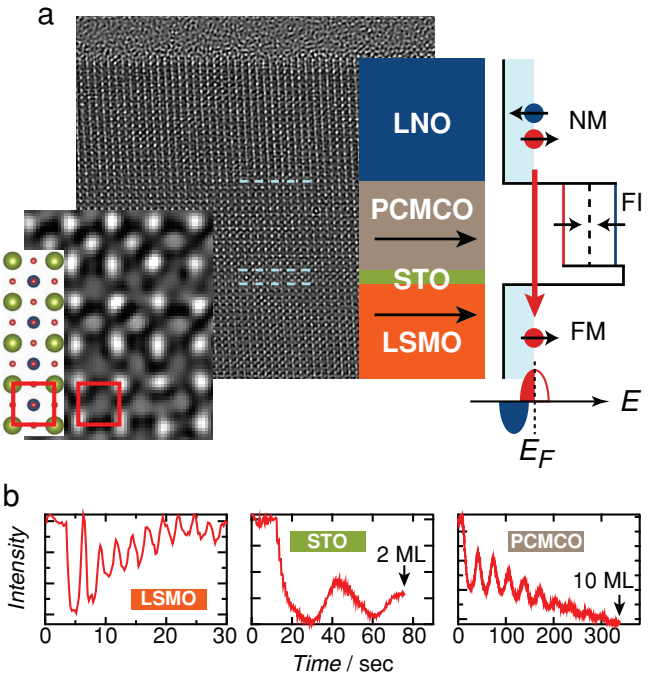

Figure 1. Device structure and crystal growth. a) The HR-TEM image of the LNO/PCMCO ($y = 0.2$)/STO/LSMO SFTJ and a simplified band diagram. Interfaces are indicated by blue broken lines in the HR-TEM image. The inset shows an enlarged view of the PCMCO layer together with a model of the ABO_3 perovskite crystal structure (A: green circles, B: blue circles, O: red dots). The perovskite unit cell is marked by red squares. In the band diagram, the tunnel barrier heights for the up-spin (down-spin) electrons are indicated by the red (blue) lines. b) The RHEED oscillation during the growth of LSMO (left), STO (middle), and PCMCO (right) layers. Each oscillation corresponds to the growth of a single perovskite unit cell layer (1 ML).

In this work, a large TMR signal, exceeding 120% in an epitaxial oxide SFTJ, was achieved by severing the magnetic coupling between the spin filter layer and the ferromagnetic electrode. The tunnel barrier was made of a perovskite-type oxide, $Pr_{0.8}Ca_{0.2}Mn_{1-y}Co_yO_3$ (PCMCO),[14] which shows robust ferromagnetism for $y = 0$–0.3, even in very thin layers, while retaining insulating properties. As we have previously reported,[14] the magnetic properties of PCMCO thin films are dependent on the Co content. The Curie temperature and saturation magnetization are enhanced by increasing the Co content up to y = 0.3. The band gap of the base compound, $Pr_{0.8}Ca_{0.2}MnO_3$ can be assumed to be just under 1 eV, considering the typical band gap of similar perovskite manganites.[15] The order of the resistivity is basically constant independent of the Co content. From the view point of device construction, the controllable magnetic hardness of PCMCO is found to be useful for designing multi-spin-filter tunnel devices that are composed of more than two consecutive spin filters, e.g., NM/FI/NI/FI/NM or NM/FI/NM/FI/NM junctions.[8,16] The results of this work open the possibility of designing novel spintronic devices, such as spin resonant tunneling diodes[16,17] or spin hot electron transistors[18] using spin filter tunnel barriers as building blocks.

2. Results and Discussion

2.1. Control of Magnetic Coupling

The structure of the SFTJ developed in this work is shown in Figure 1a. In this structure, electrons injected from the $LaNiO_3$ (LNO) (20 ML) normal-metal electrode were filtered by a PCMCO spin filter tunnel barrier (10–12 ML). The thickness of each layer is noted in terms of the perovskite unit cell height, for which 1 ML, ≈0.4 nm. Film thickness was controlled by counting the oscillations of the reflection high-energy electron diffraction (RHEED) intensity as shown in Figure 1b. Due to the exchange splitting in the PCMCO layer, up-spin electrons selectively tunnel through the tunnel barrier (Figure 1a, right). The resultant spin-polarized current can be detected by a $La_{0.6}Sr_{0.4}MnO_3$ (LSMO) (250 ML) ferromagnetic electrode as a TMR signal. If the ferromagnetic properties of the PCMCO and LSMO layers are retained near the interface, these two layers will be magnetically coupled through magnetic interactions, which will hinder the detection of the spin-polarized current as a TMR signal. In order to magnetically decouple the thick LSMO spin detector from the PCMCO spin filter, a nonmagnetic insulator $SrTiO_3$ (STO) (2 ML) was inserted between the two layers.

The state-of-the-art epitaxial growth technique yielded atomically abrupt interfaces, as shown in the high-resolution transmission electron microscope (HR-TEM) image of a LNO/PCMCO (y = 0.2)/STO/LSMO junction in Figure 1a, left. The dominant conduction mechanism of the SFTJ was confirmed to be tunneling from the current-voltage characteristics shown in the Supporting Information. Both PCMCO (10 ML) and LSMO (20 ML) films showed a clear ferromagnetic response, as seen from the magnetic field dependences of the magnetization (M-H curves) in **Figure 2**a,b. When these layers were combined, a single-step M-H curve was observed, as shown in Figure 2c, blue dotted line. This means that the magnetizations in the PCMCO and LSMO layers were reversed simultaneously due to magnetic coupling between the layers. The existence of the magnetic coupling is evidence that the PCMCO tunnel barrier and the LSMO electrode maintained robust ferromagnetism even at the PCMCO/LSMO interface. However, the magnetic coupling also reduces the TMR ratio because it prevents the PCMCO and LSMO layers from being independently switched to either a parallel or anti-parallel magnetic configuration. It is thus important to cut the magnetic coupling by inserting a nonmagnetic layer.[2] For this purpose, a thin nonmagnetic insulator STO (2 ML) was inserted at the PCMCO/LSMO interface, resulting in independent magnetization reversals of the PCMCO and LSMO layers. The M-H curve of a PCMCO/STO (2 ML)/LSMO structure (Figure 2c, red line) does indeed show a two-step hysteresis curve, corresponding to independent reversals of the magnetizations in PCMCO (purple arrows) and LSMO (black arrow).[19] The effect of the magnetic coupling can be seen in the low-field region of the M-H curves. The magnetic field for magnetization reversal of LSMO (H_{LSMO}) is larger without the presence of the STO spacer layer (Figure 2c, blue line) than with STO (Figure 2c, red line). This indicates that the magnetic coupling between PCMCO and LSMO is ferromagnetic. In

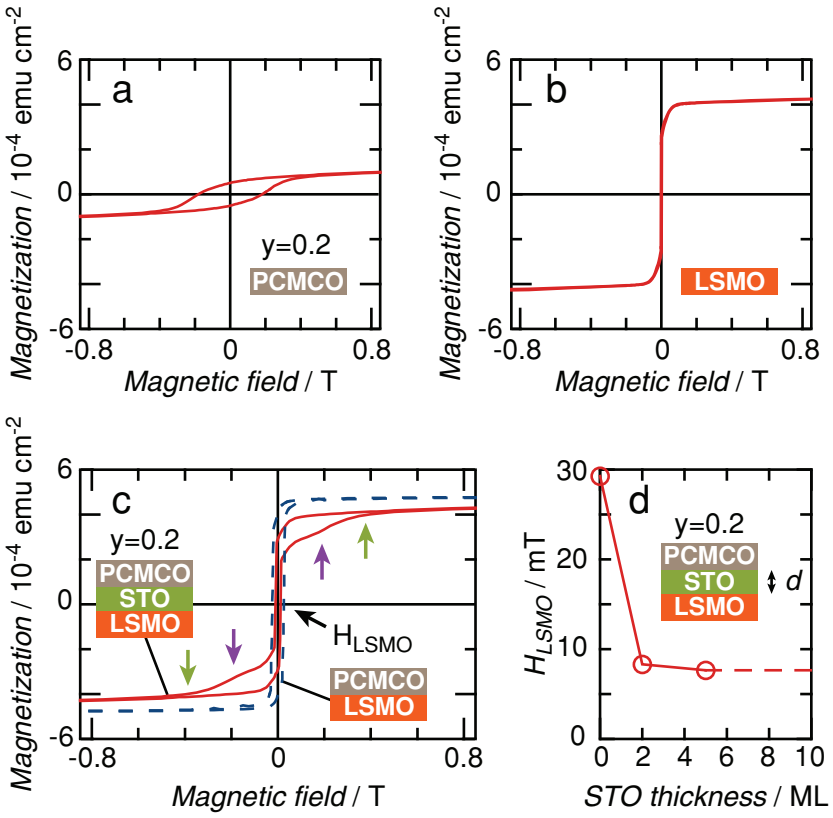

Figure 2. Magnetic properties of the spin filter tunnel junctions. The M-H curves of a) PCMCO ($\gamma = 0.2$) and b) LSMO single layers. c) Comparison of M-H curves of PCMCO ($\gamma = 0.2$) (10 ML)/STO(2 ML)/LSMO(20 ML) (red solid line) and PCMCO ($\gamma = 0.2$) (10 ML)/LSMO(20 ML) (blue dotted line) heterostructures. H_{LSMO} and the saturation magnetic field H_S (M-H) are indicated by black and green arrows, respectively. The step structures corresponding to the magnetization reversals in PCMCO are marked with purple arrows. d) The STO thickness dependence of H_{LSMO} in PCMCO ($\gamma = 0.2$) (10 ML)/STO/LSMO(20 ML) heterostructures. All the M-H curves are measured at 10 K. The dotted line marks the H_{LSMO} value for the 250 ML STO layer.

order to determine the minimum thickness of the nonmagnetic STO layer that is needed to break the ferromagnetic coupling, a STO thickness dependence of H_{LSMO} was measured, as plotted in Figure 2d. The plot shows that by inserting 2 MLs of STO, H_{LSMO} dropped almost to the bulk value of 5 mT and remained constant even if the STO thickness was increased to 250 ML, suggesting that the 2 MLs of STO is sufficient to decouple the ferromagnetic interaction between PCMCO and LSMO.

2.2. Observation of Spin Filtering Effect

The operation of a spin filter can be verified by observing the magnetic field dependence of the junction resistance (TMR curve), as shown in **Figure 3**a,b. In a LNO/PCMCO(10 ML)/LSMO reference structure (Figure 3a), no TMR response was observed because the ferromagnetic coupling between the PCMCO and LSMO layers prevented independent magnetization reversals in the two layers. Inserting a 2 ML STO spacer layer, as shown in Figure 3b, led to a large and clear TMR response that exceeded 120%. According to the extended Jullière model,[20] TMR can be expressed as $TMR = 2P_{SF}P_{SD}/(1 - P_{SF}P_{SD})$, where P_{SF} and P_{SD} are the efficiency of the spin filtering and spin detection, respectively. Using this formula, the spin polarization of the tunneling electrons from a LNO electrode through a PCMCO spin filter can be estimated to be $P_{SF} = 42\%$, assuming the spin polarization of the STO/LSMO interface to be $P_{SD} = 90\%$.[21]

In a spin filter tunnel junction, the width of the TMR curve (H_S (MR), **Figure 4** inset) should coincide with the saturation magnetic field of the PCMCO layer determined from the M-H curve (H_S (M-H), Figure 4 inset). In order to confirm this, H_S (MR) is plotted together with H_S (M-H) for various Co substitution levels γ in the PCMCO layer in Figure 4. By increasing the Co content in the PCMCO layer, H_S (M-H) increased from 0.1 T at $\gamma = 0$ to 0.9 T at $\gamma = 0.3$ due to the presence of the Co ions that increase the magnetic hardness of PCMCO.[14] The H_S (MR) and H_S (M-H) curves showed good agreement for all Co substitution levels up to $\gamma = 0.3$ (Figure 4). This means that the hysteresis observed in Figure 3b originated from the spin filtering effect in the PCMCO layer and is not related to other factors such as domain formation in LSMO.[22]

2.3. Multi-Spin-Filter Tunneling Devices

The controllable magnetic hardness of PCMCO, demonstrated in Figure 4, offers an excellent platform for building novel spintronic devices by embedding spin filters into multibarrier tunnel devices, such as spin resonant tunneling diodes[16,17] or spin hot-electron field-effect transistors.[18] When using more than two spin filter layers in one device, it is necessary to switch the magnetic orientation of each spin filter layer independently. It is thus essential to use a ferromagnetic insulator with different magnetic hardness for each spin filter layer. However, as the choice of available ferromagnetic insulator materials is quite limited, it would be difficult to fabricate multi-spin-filter tunneling devices[8] by combining two different spin filter materials. By using PCMCO spin filter layers, it is possible to design multi-spin-filter tunneling devices by systematically varying the Co content of each spin filter layer.

This approach is demonstrated here by constructing a double-spin-filter tunnel junction (NM/FI/NI/FI/NM) with a device structure shown in **Figure 5**a. In earlier work, two EuS spin filter layers grown under different conditions have been used in EuS/Al_2O_3/EuS double-spin-filter tunnel junctions to get a sufficient coercive field difference.[8] In this work, two PCMCO spin filter layers with different Co contents ($\gamma = 0$ and $\gamma = 0.2$) are used for two independently-controllable spin filter layers, separated by a STO spacer layer that magnetically decouples the two spin filter layers. This device can exhibit a TMR signal

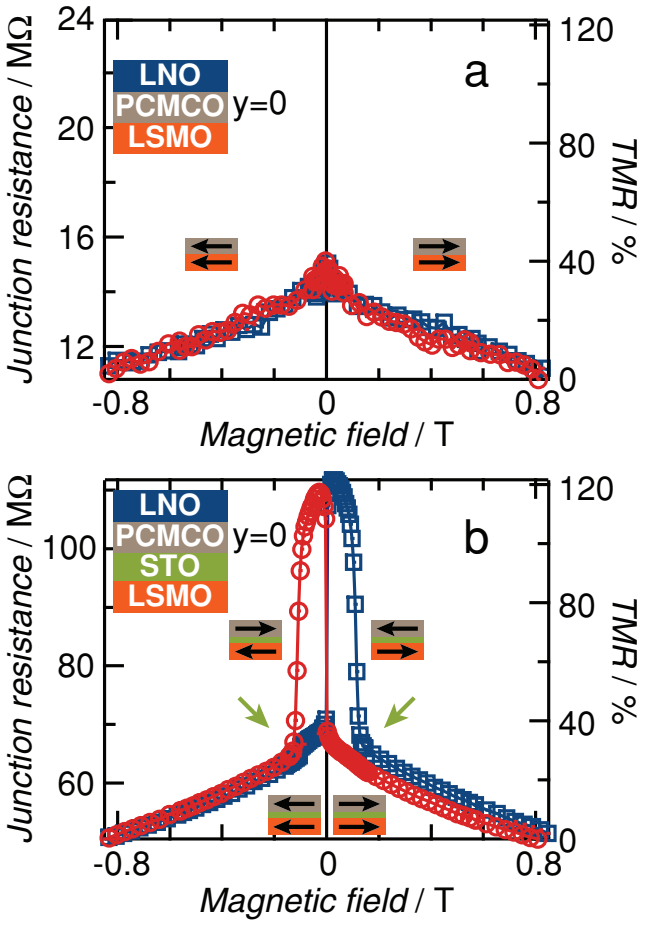

Figure 3. TMR response of the spin filter tunnel junctions. a) LNO/PCMCO (γ = 0)(10 ML)/LSMO and b) LNO/PCMCO (γ = 0)(10 ML)/STO(2 ML)/LSMO junctions. The TMR curves are measured at 4 K. The saturation magnetic field H_S (MR) is indicated by green arrows

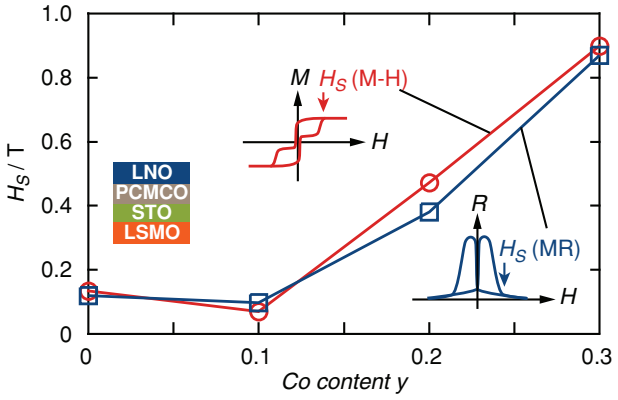

Figure 4. Comparison of the saturation magnetic fields determined from the M-H and TMR curves for various Co substitution levels in the PCMCO layer.

without any ferromagnetic (FM) spin detector electrodes. The operating principle is based on the magnetization-dependent tunnel barrier height in the PCMCO/STO/PCMCO tunnel barrier. As shown in the simplified band diagram in Figure 5a, when the magnetic orientations of the two PCMCO layers are parallel (P), the up-spin electrons can selectively tunnel through the barrier seeing two lower tunnel barrier heights in both PCMCO layers (red lines in the band diagram), while the down-spin electrons see two higher tunnel barrier heights (blue lines in the band diagram). When the magnetic orientations of the PCMCO layers are antiparallel (AP), the up-spin and down-spin electrons need to tunnel through one lower tunnel barrier and one higher tunnel barrier in two PCMCO layers. The total tunneling current can be calculated by summing the up-spin and down-spin currents, which becomes larger in the parallel state than the antiparallel state. The magnetic field dependence of the junction resistance clearly showed a TMR signal that results from the parallel and antiparallel magnetic configurations of PCMCO (γ = 0.2) and PCMCO (γ = 0) spin filter layers as shown in Figure 5b. Successful operation of the double-barrier device shows that it is possible to construct spintronic junctions that do not rely on ferromagnetic metals. The resistance of the double-spin-filter tunnel junction is smaller than that of the single-spin-filter tunnel junction shown in Figure 3b due to a larger roughness of the LNO bottom electrode, which decreases the effective tunnel barrier thickness and makes the device performance dependent on the bottom electrode flatness.

3. Conclusion

In summary, we have demonstrated that SFTJs based on a PCMCO FI tunnel barrier can function as a highly efficient source of spin-polarized electrons. By magnetically decoupling the PCMCO spin filter from a LSMO spin detector with a nonmagnetic STO layer, a clear TMR effect exceeding 120% was achieved. We also show that the magnetic hardness of PCMCO can be accurately tuned by suitable Co substitution, making it

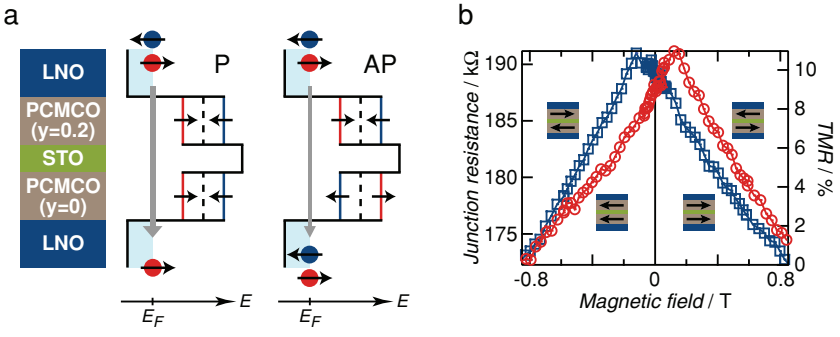

Figure 5. Operation of the double spin filter tunnel junction. a) Device structure and a simplified band diagram for the parallel state (P) and antiparallel state (AP). b) TMR curve of a LNO/PCMCO (γ = 0.2) (6 ML)/STO (2 ML)/PCMCO (γ = 0) (6 ML)/LNO double spin filter tunnel junction measured at 4 K.

possible to design multi-spin-filter tunneling devices that do not require the presence of ferromagnetic metals. This work demonstrates the importance of atomic-layer level control of epitaxial oxide thin film growth for constructing high-performance spintronic devices. Further study for example on PCMCO thickness dependence of the TMR response would be important to achieve better device performance[25] and to investigate coherence of the tunneling electrons, as reported in single-crystalline TMR junctions.[26]

4. Experimental Section

Device Fabrication: Epitaxial NM/FI/NI/FM multilayers composed of LNO/PCMCO/STO/LSMO, schematically illustrated in Figure 1a, were fabricated on atomically flat (001)-oriented STO substrates (Shinkosha, Co., LTD) by pulsed laser deposition. A λ = 248 nm KrF excimer laser (Tui Laser, Thin Film Star) was used for ablation. The LSMO layer was grown at a substrate temperature of 900 °C under an oxygen pressure of 0.08 Pa.[23] The ablation fluence was 0.55 J/cm^2 at a pulse repetition rate of 5 Hz. The STO, PCMCO, and LNO layers were grown at a substrate temperature of 700 °C under an oxygen pressure of 4 Pa in the laser ablation condition of 0.94–1.14 J/cm^2, 1 Hz.[14,24] The PCMCO/STO tunnel barrier thickness was controlled by monitoring oscillations of the RHEED specular intensity as shown in Figure 1b. The layered structures were patterned using conventional photolithography and Ar ion milling. The junction area was 8×32 μm^2. Poly-Au top electrodes for contact pads were made by standard vacuum evaporation. After dry etching by Ar ion milling, the entire devices were annealed at 500 °C in air for 24 h to reduce the density of oxygen vacancies formed in the dry etching process.

Device Characterization: The magnetic field dependences of the junction resistance were measured at 4 K by cooling the junctions using an Oxford Microstat He cryostat. The junction resistance was measured using a Keithley 6517A electrometer by applying a DC bias voltage of 5 mV with a Keithley 2635 sourcemeter in a magnetic field generated by a conventional electromagnet. The magnetic properties of the unpatterned films were characterized using a Quantum Design Magnetic Properties Measurement System (MPMS).

Supporting Information

Supporting Information is available from the Wiley Online Library or from the author.

Acknowledgements

The authors acknowledge Prof. T. Hasegawa for MPMS measurements. This work was supported by a Grant-in-Aid for Scientific Research 22015006, 20047003. T.H. acknowledges financial support from JSPS.

Received: April 6, 2012
Revised: June 1, 2012
Published online: July 2, 2012

[1] J. S. Moodera, X. Hao, G. A. Gibson, R. Meservey, *Phys. Rev. Lett.* **1988**, *61*, 637.
[2] M. Gajek, M. Bibes, S. Fusil, K. Bouzehouane, J. Fontcuberta, A. Barthélémy, A. Fert, *Nat. Mater.* **2007**, *6*, 296.
[3] a) Z. Sefrioui, C. Visani, M. J. Calderón, K. March, C. Carrétéro, M. Walls, A. Rivera-Calzada, C. León, R. L. Anton, T. R. Charlton, F. A. Cuellar, E. Iborra, F. Ott, D. Imhoff, L. Brey, M. Bibes, J. Santamaria, A. Barthélémy, *Adv. Mater.* **2010**, *22*, 5029; b) E. Y. Tsymbal, H. Kohlstedt, *Science* **2006**, *313*, 181; c) A. Gruverman, D. Wu, H. Lu, Y. Wang, H. W. Jang, C. M. Folkman, M. Y. Zhuravlev, D. Felker, M. Rzchowski, C. B. Eom, E. Y. Tsymbal, *Nano Lett.* **2009**, *9*, 3539; d) M. Hambe, A. Petraru, N. A. Pertsev, P. Munroe, V. Nagarajan, H. Kohlstedt, *Adv. Funct. Mater.* **2010**, *20*, 2436.
[4] J. S. Moodera, R. Meservey, X. Hao, *Phys. Rev. Lett.* **1993**, *70*, 853.
[5] a) P. LeClair, J. K. Ha, H. J. M. Swagten, J. T. Kohlhepp, C. H. van de Vin, W. J. M. de Jonge, *Appl. Phys. Lett.* **2002**, *80*, 625; b) B. B. Nelson-Cheeseman, R. V. Chopdekar, L. M. B. Alldredge, J. S. Bettinger, E. Arenholz, Y. Suzuki, *Phys. Rev. B* **2007**, *76*, 220410; c) A. V. Ramos, M.-J. Guittet, J.-B. Moussy, R. Mattana, C. Deranlot, F. Petroff, C. Gatel, *Appl. Phys. Lett.* **2007**, *91*, 122107; d) Y. K. Takahashi, S. Kasai, T. Furubayashi, S. Mitani, K. Inomata, K. Hono, *Appl. Phys. Lett.* **2010**, *96*, 072512.
[6] A. T. Filip, P. LeClair, C. J. P. Smits, J. T. Kohlhepp, H. J. M. Swagten, B. Koopmans, W. J. M. de Jonge, *Appl. Phys. Lett.* **2002**, *81*, 1815.
[7] a) M. G. Chapline, S. X. Wang, *Phys. Rev. B* **2006**, *74*, 014418; b) U. Lüders, A. Barthélémy, M. Bibes, K. Bouzehouane, S. Fusil, E. Jacquet, J.-P. Contour, J.-F. Bobo, J. Fontcuberta, A. Fert, *Adv. Mater.* **2006**, *18*, 1733.
[8] G.-X. Miao, M. Müller, J. S. Moodera, *Phys. Rev. Lett.* **2009**, *102*, 076601.
[9] E. Wada, K. Watanabe, Y. Shirahata, M. Itoh, M. Yamaguchi, T. Taniyama, *Appl. Phys. Lett.* **2010**, *96*, 102510.
[10] a) G. Schmidt, D. Ferrand, L. W. Molenkamp, A. T. Filip, B. J. van Wees, *Phys. Rev. B* **2000**, *62*, R4790; b) E. I. Rashba, *Phys. Rev. B* **2000**, *62*, R16267.
[11] T. S. Santos, J. S. Moodera, *Phys. Rev. B* **2004**, *69*, 241203.
[12] M. Gajek, M. Bibes, A. Barthélémy, K. Bouzehouane, S. Fusil, M. Varela, J. Fontcuberta, A. Fert, *Phys. Rev. B* **2005**, *72*, 020406.
[13] T. S. Santos, J. S. Moodera, K. V. Raman, E. Negusse, J. Holroyd, J. Dvorak, M. Liberati, Y. U. Idzerda, E. Arenholz, *Phys. Rev. Lett.* **2008**, *101*, 147201.
[14] T. Harada, I. Ohkubo, M. Lippmaa, Y. Matsumoto, M. Sumiya, H. Koinuma, M. Oshima, *Phys. Status Solidi RRL* **2011**, *5*, 34.
[15] M. K. Dalai, P. Pal, B. R. Sekhar, N. L. Saini, R. K. Singhal, K. B. Garg, B. Doyle, S. Nannarone, C. Martin, F. Studer, *Phys. Rev. B* **2006**, *74*, 165119
[16] A. Saffarzadeh, *J. Phys. Condens. Mater.* **2003**, *15*, 3041.
[17] A. Iovan, S. Andersson, Y. G. Naidyuk, A. Vedyaev, B. Dieny, V. Korenivski, *Nano Lett.* **2008**, *8*, 805.
[18] a) S. Sugahara, M. Tanaka, *Physica E* **2004**, *21*, 996; b) T. Yajima, Y. Hikita, H. Y. Hwang, *Nat. Mater.* **2011**, *10*, 198.
[19] A. M. Sánchez, L. Äkäslompolo, Q. H. Qin, S. van Dijken, *Cryst. Growth Des.* **2012**, *12*, 954.
[20] M. Jullière, *Phys. Lett. A* **1975**, *54*, 225.
[21] a) R. J. Soulen, J. M. Byers, M. S. Osofsky, B. Nadgorny, T. Ambrose, S. F. Cheng, P. R. Broussard, C. T. Tanaka, J. Nowak, J. S. Moodera, A. Barry, J. M. D. Coey, *Science* **1998**, *282*, 85; b) M. Bowen, M. Bibes, A. Barthélémy, J.-P. Contour, A. Anane, Y. Lemaitre, A. Fert, *Appl. Phys. Lett.* **2003**, *82*, 233; c) V. Garcia, M. Bibes, A. Barthélémy, M. Bowen, E. Jacquet, J. P. Contour, A. Fert, *Phys. Rev. B* **2004**, *69*, 052403.
[22] C. Gould, C. Rüster, T. Jungwirth, E. Girgis, G. M. Schott, R. Giraud, K. Brunner, G. Schmidt, L. W. Molenkamp, *Phys. Rev. Lett.* **2004**, *93*, 117203.
[23] T. Harada, I. Ohkubo, M. Oshima, *Mater. Trans.* **2009**, *50*, 1081.
[24] K. Tsubouchi, I. Ohkubo, H. Kumigashira, Y. Matsumoto, T. Ohnishi, M. Lippmaa, H. Koinuma, M. Oshima, *Appl. Phys. Lett.* **2008**, *92*, 262109.
[25] C. W. Miller, *J. Magn. Magn. Mater.* **2009**, *321*, 2563.
[26] S. Yuasa, T. Nagahama, A. Fukushima, Y. Suzuki, K. Ando, *Nat. Mater.* **2004**, *3*, 868.